High fidelity quantum memory via dynamical decoupling: theory and experiment

Xinhua Peng[1,3], Dieter Suter[1] and Daniel A Lidar[2]

[1] Department of Physics, Technische Universität Dortmund, Germany
[2] Departments of Electrical Engineering, Chemistry, and Physics, Center for Quantum Information Science & Technology, University of Southern California, Los Angeles, CA 90089, USA
[3] Hefei National Laboratory for Physical Sciences at Microscale and Department of Modern Physics, University of Science and Technology of China, Hefei, Anhui 230026, People's Republic of China

E-mail: lidar@usc.edu

Abstract

Quantum information processing requires overcoming decoherence—the loss of 'quantumness' due to the inevitable interaction between the quantum system and its environment. One approach towards a solution is quantum dynamical decoupling—a method employing strong and frequent pulses applied to the qubits. Here we report on the first experimental test of the concatenated dynamical decoupling (CDD) scheme, which invokes recursively constructed pulse sequences. Using nuclear magnetic resonance, we demonstrate a near order of magnitude improvement in the decay time of stored quantum states. In conjunction with recent results on high fidelity quantum gates using CDD, our results suggest that quantum dynamical decoupling should be used as a first layer of defense against decoherence in quantum information processing implementations, and can be a stand-alone solution in the right parameter regime.

1. Introduction

One of the main difficulties in the implementation of quantum information processing is the susceptibility of quantum systems to interactions with their environment. Any such uncontrolled interaction degrades the quantum information stored in the system; in the present context, this process is known as decoherence [1]. When a quantum system performs an information processing task, decoherence causes computational errors, which leads to the eventual loss of any quantum advantage in information processing [2]. Dynamical decoupling (DD) is a form of quantum error *suppression* that modifies the system-environment interaction so that its overall effects are very nearly self-cancelling, thereby decoupling the system evolution from that of the decoherence-inducing environment [3, 4]. DD has been primarily studied as a specialized quantum control technique for state preservation, or 'quantum memory' . In this setting it has been demonstrated theoretically that DD is capable of generating long-lived and robust quantum states. Three recently introduced techniques

have figured most prominently in this effort: 'randomized DD' (RDD), [5] 'concatenated DD' (CDD) [6] and 'Uhrig DD' (UDD) [7]. RDD, which involves randomly selected pulse types applied at regular intervals, works best for strongly time-dependent environments and in the long time limit [8, 9]. UDD, which involves an optimization of pulse intervals for a fixed pulse type, is provably optimal for the restricted case of a single qubit with diagonal coupling to the environment [10, 11]. UDD has been the subject of extensive recent experimental tests. Following some notable successes [12–14], the general picture emerging is that UDD performance depends sensitively on the existence of a sharp high-frequency cutoff; in the absence of such a cutoff simpler DD schemes tend to result in better performance [15–17]. UDD was recently extended to 'quadratic DD' (QDD) which applies to general environments, but is still limited to only a single qubit [18]. Very recently a generalization of QDD to multiple qubits was proposed, which involves a higher order nesting of UDD sequences [19]. CDD is a method for constructing pulse sequences with a recursive

structure. While CDD requires longer pulse sequences than UDD and QDD, there is strong theoretical evidence that it can be successfully combined with quantum computation and incorporated into quantum logic circuits [20, 21]. For this reason we focus here on CDD, and present the first experimental evidence, using nuclear magnetic resonance (NMR) techniques, for the theoretically predicted advantage [6, 9, 20–24] of using CDD for quantum memory preservation over its common counterpart 'periodic dynamical decoupling' (PDD)[4]. We also provide a theoretical analysis in support of these experimental results. Although our experimental results illustrate the effectiveness of CDD specifically for NMR, the CDD framework is generally applicable to any decohering quantum system. Our results lend support to the expectation that DD will prove an indispensable tool in scalable quantum information processing.

2. DD and CDD

We consider a system described by a Hamiltonian

$$H = H_S + H_B + H_{SB}, \qquad (1)$$

where H_S acts on the system degrees of freedom, H_B on the environment and H_{SB} couples the system to the environment. To suppress errors, DD allows the system to evolve for some time before applying a control pulse to redirect or refocus the evolution towards the error-free ideal, continually repeating this process until some total evolution has completed:

$$\text{DD}[U(\tau)] = P_N U(\tau_0) \cdots P_2 U(\tau_0) P_1 U(\tau_0) = \widetilde{U}(N\tau_0), \quad (2)$$

where $U(\tau_0) = U_0(\tau_0)B(\tau_0)$ represents the unitary evolution of the combined system and environment, or bath, for a duration of length τ_0, decomposed so that $U_0(\tau_0)$ determines the ideal, desired error-free evolution generated by a piece-wise constant system Hamiltonian H_S, and $B(\tau_0)$ is a unitary error operator acting jointly on the system and bath. We use the symbol $\widetilde{U}$ to denote evolution in the presence of DD pulses. For now, we implicitly assume that the pulses P_j are sufficiently fast as to not contribute to the total time of the evolution. This assumption is not essential, but is useful in simplifying our present discussion. The simplest example is quantum memory, where $U_0(\tau_0) = I_S$ is the identity operation or 'free evolution' of the system, and $B(\tau_0)$ represents the deviation from the ideal dynamics caused by the presence of a bath. In this case, our goal is to choose pulses so that $\text{DD}[U(\tau)] = I_S \otimes \widetilde{B}$, the identity acting on the system and an arbitrary pure bath operator $\widetilde{B}$. DD schemes differ in precisely how these pulses P_j are chosen, with the only common constraint that the following basic 'decoupling condition' is met [3, 4]:

$$\sum_\alpha P_\alpha^\dagger H_{SB} P_\alpha = 0. \qquad (3)$$

To be concrete, we will suppose that the pulses $P_\alpha \in \{I, X, Y, Z\}$ are Pauli operators, though again this assumption only serves to keep the explanation simple and is not strictly

necessary. CDD generates pulse sequences by *recursively* building on a base sequence $Z[\cdot]X[\cdot]Z[\cdot]X[\cdot]$ (or any other ordered pair of Pauli operators from the set $\{X, Y, Z\}$) as follows. The sequence is initialized as

$$\text{CDD}_0[U(\tau_0)] = U(\tau_0) = U_0(\tau_0)B(\tau_0) \equiv \widetilde{U}_0(\tau_0), \qquad (4)$$

and higher levels are generated via the rule

$$\begin{aligned}
\widetilde{U}_{n+1}(\tau_{n+1}) &\equiv \text{CDD}_{n+1}[U(\tau_0)] \\
&= Z[\widetilde{U}_n(\tau_n)]X[\widetilde{U}_n(\tau_n)]Z[\widetilde{U}_n(\tau_n)]X[\widetilde{U}_n(\tau_n)], \quad (5)
\end{aligned}$$

where $\tau_n = 4^n \tau_0$. Thus, at each level the total duration of the CDD pulse sequence grows by a factor of 4, while the pulse interval remains fixed at its initial value τ_0. Note that we are allowing for the possibility of some non-trivial information processing operation $U_0(\tau_0)$, as implemented in [21]. The choice of the base sequence is motivated by the observation that it satisfies the 'decoupling condition' (3) in the quantum memory setting $U_0(\tau_0) = I_S$, under the dominant '1-local' system-bath coupling term $H_{SB}^{(1)} = \sum_{\alpha=x,y,z} \sum_j \sigma_j^\alpha \otimes B_j^\alpha$, where $\sigma_j^x \equiv X, \sigma_j^y \equiv Y$, and $\sigma_j^z \equiv Z$ denote the Pauli matrices acting on the system qubit j, and $\{B_j^\alpha\}$ are arbitrary bath operators. (The next order '2-local' coupling would have terms such as $\sigma_j^\alpha \sigma_k^\beta \otimes B_{jk}^{\alpha\beta}$, etc.) For this reason the base sequence is sometimes called the 'universal decoupler'. Similarly, the most common pulse sequence used thus far in DD experiments is 'periodic DD' (PDD), which generates pulse sequences by *periodically* repeating the universal decoupler base sequence $Z[\cdot]X[\cdot]Z[\cdot]X[\cdot]$:

$$\text{PDD}_k[U(\tau_0)] = (\text{PDD}_1[U(\tau_0)])^k = \widetilde{U}_k(4k\tau_0), \qquad (6)$$

where $\text{PDD}_1[U(\tau_0)] = \text{CDD}_1[U(\tau_0)]$. Note that in equation (6) $\widetilde{U}_k$ refers to the *k*-fold *repetition* of single cycles of the sequence, while in equation (5) $\widetilde{U}_n$ describes the *n*-fold *concatenation* of identical cycles.

The use of periodic pulse sequences has a long history, starting with some of the earliest spin-echo experiments [29]. Indeed, it is natural to try to design a 'good' pulse sequence and then repeat it over and over again so as to cover a desired total experiment time *T*. CDD breaks with this intuition and tradition, by demanding that a different pulse sequence be used for every given *T*: given a feasible pulse interval τ_0, the appropriate CDD order *n* is found from the condition $T = 4^n \tau_0$. Unlike in PDD, the pulse order in CDD level $n + 1$ is completely different from that in level *n*. However, in our experiments we also tested applying cycles of CDD of a given order (periodic CDD, or PCDD) [24].

Next we present the results of the first-ever CDD experiment[5]. The results demonstrate that, as predicted [6, 9, 20–24], CDD outperforms PDD in preserving quantum memory, and CDD becomes increasingly effective at higher concatenation levels.

---

[4] Since this work first appeared as a preprint (arXiv:0911.2398) a number of other experimental studies comparing CDD and PDD have been published [25–28].

[5] These experiments were first carried out in May 2005 in collaboration with Marko Lovric, and subsequently refined and presented in various talks given by the authors.

J. Phys. B: At. Mol. Opt. Phys. **44** (2011) 154003

X Peng *et al*
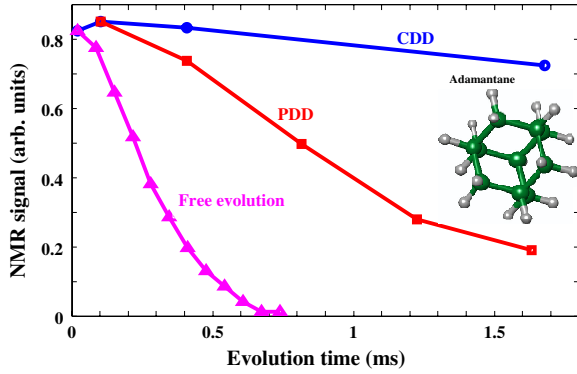
Figure 1. Experimental comparison of CDD versus PDD versus free evolution on a 300 MHz NMR spectrometer. Shown is the signal decay of the ^{13}C-spin coherence of adamantane ($C_{10}H_{16}$, depicted in the inset) versus total evolution time. The spin echo is measured by first creating the equal superposition state $(|0\rangle + |1\rangle)/\sqrt{2}$, then subjecting it to either PDD (red squares) or CDD (blue circles) pulse sequences and finally measuring the free induction decay. The first point shows the amplitude of the free induction decay signal, measured after a pulse interval of $\tau_0 = 15\,\mu$s (i.e. CDD_0, equation (4)). The second point corresponds to $CDD_1 = PDD$. The third and the fourth blue points correspond to CDD_2 and CDD_3, respectively. The width of the π-pulses was $\delta = 10.52\,\mu$s. For reference we also show the free evolution, without any pulses (triangles).

3. Experimental results on quantum memory using CDD

Presented in figures 1–3 are the results of quantum memory NMR spectroscopy experiments. The experiments were performed at TU Dortmund with a homebuilt 300 MHz solid-state NMR spectrometer using a 7.05 T Oxford magnet and a homebuilt double resonance (HC) probe. Before the experiments, we first used suitable tune-up pulse sequences [30–32] to minimize pulse-length errors and phase transients for the ^{13}C channel by adjusting the probe tuning and RF amplitudes. For the tune-up, we used a liquid sample of ^{13}C-labelled Methanol (99% enriched).

To measure the effect of the decoupling sequences, we used a sample of powdered adamantane. In this plastic crystal, the nearly spherical molecules tumble rapidly and isotropically in the solid phase. The motion averages all intramolecular dipolar couplings to zero, but does not eliminate intermolecular couplings. As a result of this averaging process, there is only one coupling between every pair of molecules, thereby reducing the adamantane molecule to a point dipole source containing 16 proton spins or 16 proton spins and one ^{13}C-nuclear spin in any C position (11% of the molecules). All remaining interactions (except for the Zeeman term) are insignificant. The sensitivity of ^{13}C NMR signals was enhanced by the standard cross-polarization experiment, which provides polarization transfer from the abundant ^{1}H spins. The enhancement factor of the ^{13}C signal was about 3.2. After the transfer, the carbon spin magnetization was stored for 2 ms as longitudinal magnetization. Another $\pi/2$ pulse created transverse ^{13}C magnetization as the initial state for the dynamic decoupling experiments.
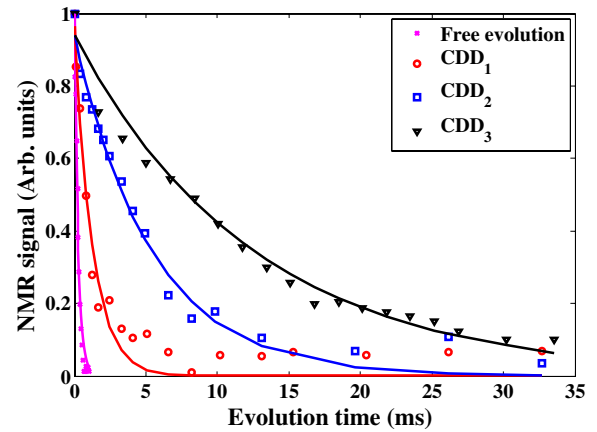
Figure 2. Signal decays of ^{13}C-spin for the free evolution, CDD_1, CDD_2 and CDD_3 with $\tau_0 = 15\,\mu$s. The solid lines denote the fitting to an exponential decay. For a given CDD order, successive data points correspond to an increasing number of CDD cycles, starting from a single cycle as in figure 1 (the PCDD protocol [24]).
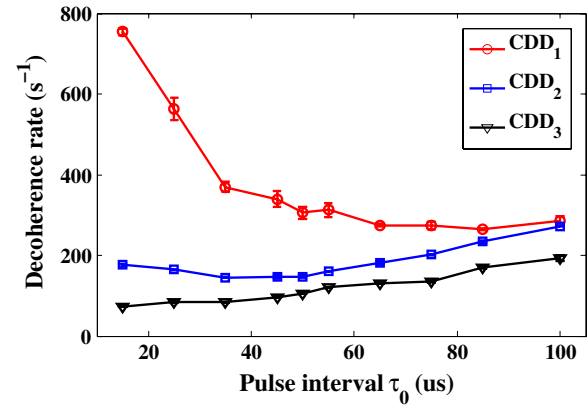
Figure 3. Decoherence rate versus pulse interval for the adamantene system shown in figure 1, for $CDD_1 = PDD_1$ (red, circles), CDD_2 (blue, squares) and CDD_3 (black, triangles). For PDD with non-ideal pulses, errors due to finite pulse-width accumulate and overwhelm the improvement due to the smaller pulse interval. CDD, on the other hand, compensates for finite pulse width errors, and hence improvement is seen with smaller pulse intervals, as expected. CDD decoherence rates were extracted from PCDD cycles as shown in figure 2.

In the experiments, the width δ of the π pulses for ^{13}C was 10.52 μs. Pairs of π pulses with the same phase and no intervening delay were omitted. For pairs of π pulses with different phases, we inserted a minimum delay $f_a = 376$ ns to change the phase of the rf-pulse. As an example, XZf (where f denotes free evolution, without pulses) was implemented as Xf_aZf. The minimum cycle time for the PDD sequence was $\tau_c^{p1} = 4(\tau_0 + \delta)$, for the even-order CDD sequences $\tau_c^{p2k} = 4\tau_c^{p2k-1} + 2f_a$ and for the odd-order CDD sequences $\tau_c^{p2k+1} = 4(\tau_c^{p2k} + \delta)$, where τ_0 is the interval between consecutive π-pulses. The remaining signal was detected by measuring the free induction decay of the ^{13}C spins while decoupling the protons after the last echo pulse and a dead-time of $\tau_d = 8.5\,\mu$s. To obtain an accurate signal amplitude, we Fourier-transformed the free induction decays and integrated the signals over the relevant frequency range.

Figure 1 shows the spin echo signal for the ^{13}C nuclear spin qubits. In each experiment, we applied sequences of π-pulses corresponding to the various CDD orders and measured the remaining signal after the end of the sequence. We plot the absolute value of the transverse magnetization, corresponding to

$$|\langle \sigma_x - i\sigma_y \rangle| = \sqrt{\text{Tr}\big[\sigma_x \rho\big(\tau_c^{p_k}\big)\big]^2 + \text{Tr}\big[\sigma_y \rho\big(\tau_c^{p_k}\big)\big]^2}, \qquad (7)$$

where the density matrix $\rho\big(\tau_c^{p_k}\big)$ represents the state of the system at the end of DD pulse sequence (either PDD or CDD, where k now represents the number of cycle repetitions (for PDD) or number of concatenations (for CDD)). In contrast to figure 1, where the results of applying only a single cycle of each CDD order is shown. Figure 2 shows the decay of the signal as the number of CDD cycles (and thus the total evolution time) increases. In these experiments, the delay between pulses was set to $\tau_0 = 15\,\mu$s. By fitting the experimental data to an exponential decay function $S = S_0 \, e^{-t/T_2}$, we extracted the decoherence rates $1/T_2$. Figure 3 shows the decoherence rates extracted from a series of experiments conducted with different pulse intervals τ_0.

These data show that (i) higher levels of CDD suppress errors more efficiently than lower levels, (ii) at high concatenation levels the benefits of CDD increase as τ_0 decreases and (iii) CDD and PCDD always and substantially outperform PDD, an improvement that becomes more pronounced as τ_0 decreases. Indeed, comparing the results for $\text{CDD}_1 = \text{PDD}$ and CDD_3 at $\tau_0 = 15\,\mu$s in figure 3, we observe an improvement of almost an order of magnitude in the decoherence rate.

We note that the decoherence here is not engineered, but instead caused by the actual dipole–dipole interactions between the ^{13}C qubit and the ^{1}H spins inherent in the adamantane molecule. We further note that the specific nature of the interaction, be it dipole–dipole, Heisenberg, or something else altogether, is inconsequential to the success of CDD. What matters is the strength of this interaction and of the internal bath couplings relative to the DD pulse interval τ_0, as will be made more explicit in the theoretical analysis, to which we now turn.

4. Theoretical analysis

We now present a theoretical interpretation of some of the results shown in figures 1–3. To allow for a generic analysis of the DD response to different bath environments and system-bath couplings, we characterize the leading-order DD behaviour for simplicity in terms of the following relevant parameters, which capture the strength or overall rate of the internal bath and system-bath dynamics, respectively: $\beta \equiv \|H_B\|$ and $J \equiv \|H_{SB}\|$.[6] The total Hamiltonian is $H = H_S + H_B + H_{SB}$. If $J \gg \beta$, then the system-bath coupling is a dominant source of error, and remains relatively stable since the internal bath dynamics are comparatively slow. In this case, DD should produce significant fidelity gains as

[6] We note that the bounds below, which involve the operator norms J and β, are undoubtedly overly pessimistic, and could be replaced by correlation functions in a more careful analysis. See, e.g., [20].

it removes the dominant error source. On the other hand, if $J < \beta$, then the system coupling to the environment induces relatively slow dynamics, while the environment itself has fast internal dynamics. In this case, minimizing the system-bath coupling will have less of an effect on the overall dynamics, so it may be considered a worst-case scenario when assessing DD performance [22].

Let us now compare the pure system state ρ_S^0 obtained in the error-free setting, where $H_{SB} = 0$ (the desired state), to the system state ρ_S resulting from the presence of a non-zero H_{SB}, but subject to the CDD pulse sequence at level n (the actual state). The appropriate distance measure, which we would like to minimize, is the trace-norm distance D, defined in the appendix. For a total evolution time $T = N\tau_0$ using $N = 4^n$ zero-width pulses, the distance D between the desired and actual states is bounded, in the 'pessimistic' regime $J < \beta$, as [20, 22, 33]

$$D\big[\rho_S(T), \rho_S^0(T)\big] \lesssim 2J\tau_0\epsilon^n, \qquad (8)$$

where $\epsilon \equiv 4\beta\tau_0 2^n$. Here ϵ plays the role of a 'threshold parameter', i.e. rapid convergence of the distance to zero in the large n limit is guaranteed if $\epsilon < 1$. This situation is reminiscent of the error threshold in quantum fault tolerance theory [34], but requires us to decrease τ_0 while the concatenation level rises, in order to mitigate the 2^n factor. In general this is undesirable since the pulse interval cannot be decreased indefinitely. Indeed, in each of our experiments the pulse interval was fixed and the total time was variable. The interval length was varied from experiment to experiment, and the total time was adjusted accordingly, depending on the number of pulses used. Therefore, we next analyse the above bound on D under the assumption of a fixed pulse interval τ_0. We show that, perhaps counterintuitively, there is a regime where increasing the concatenation level, and hence also the total evolution time, actually leads to improved fidelity. Such an improvement can, however, not continue indefinitely, and we find that there is an optimal concatenation level beyond which fidelity starts to drop.

If δ^* is the desired maximum probability of distinguishing $\rho_S(T)$ from $\rho_S^0(T)$, we can set the bound (8) on D equal to δ^*. This yields a quadratic equation in the number of concatenation levels n, whose physically meaningful branch is

$$n = -\sqrt{[1 + \log_4(\beta\tau_0)]^2 - 2\log_4(J\tau_0/\delta^*) - 1} \\ - [1 + \log_4(\beta\tau_0)]. \qquad (9)$$

(Rounding to the nearest integer is implied.) This quantifies the 'simulation overhead' in CDD (the analogue of the poly-logarithmic simulation overhead in fault tolerance theory [34]), and means that using CDD, in the limit of zero-width pulses, we can obtain a given simulation accuracy target δ^* with a number of concatenation levels that scales only *logarithmically* in $\beta\tau_0$, $J\tau_0$ and δ^*. We can also minimize the bound (8) on D for n at fixed $J\tau_0$ and $\beta\tau_0$. The result is

$$n_{\text{opt}} = \left\lfloor \log_4 \frac{1}{\beta\tau_0} - 1 \right\rfloor, \qquad (10)$$

which is the optimal number of concatenation levels, in agreement with more involved derivations [20, 22]. At this

optimal value, which increases with decreasing $\beta\tau_0$, the bound on D scales as $e^{-\frac{1}{2}(\log_4 \beta\tau_0)^2}$ and also becomes very small in the small $\beta\tau_0$ limit. Since the internal bath dynamics are the dominant error source here, it is not surprising that the optimal concatenation level only depends on $\beta\tau_0$. A similar expression for optimal concatenation level occurs in the 'optimistic' $J > \beta$ regime, depending on both J and β [20, 22]. The key point is that even in the simplest case: ideal, single-qubit quantum memory, there exists an optimal concatenation level depending on the $J\tau_0$ and $\beta\tau_0$ parameters, after which point increasing concatenation no longer improves system fidelity. Intuitively, this optimal concatenation level represents the turning point between the competing processes of improved CDD error suppression and the exponentially increasing time for error-prone evolution that occurs with each level of concatenation. The precise point at which DD error suppression is overcome by the accumulated error depends on the relative strengths of the error-inducing Hamiltonians, determined by $J\tau_0$ and $\beta\tau_0$. For comparison, let us also consider the case of PDD with N pulses. In this case the bound $D[\rho_S(T), \rho_S^0(T)] \lesssim 2NJ\tau_0\beta\tau_0$ applies under the same assumptions as those required for the CDD bound (8) on D. The evidently much more rapid convergence of CDD, as long as pulse intervals shorter than $1/(2^{n+2}\beta)$ are attainable (the $\epsilon < 1$ condition), is due to its recursive structure, which allows CDD to cancel successive orders of the system-bath propagator in time-dependent perturbation theory [20, 22].

Returning now to our experimental CDD results (figure 3), which are in the 'pessimistic' regime $J < \beta$,[7] we see that for CDD_3 they agree with the theoretical prediction that under concatenation, lowering τ_0 improves the fidelity[8]. Moreover, they are consistent with the $\epsilon < 1$ regime, where CDD outperforms PDD. However, as can be seen in figure 1, while CDD consistently outperforms PDD, and both are better than free (unprotected) evolution, the performance of both PDD and CDD deteriorates with increasing total experiment time T. Thus, our experiments have $n_{opt} = 1$ in the sense of the optimal concatenation level of equation (10). In other words, our experiments did not reach the 'sweet spot' where a higher level of concatenation (and hence total evolution time) actually leads to increased fidelity, which would lead to $n_{opt} > 1$. The closeness of ϵ to 1 and the finiteness of the pulse width play a role in this regard.

5. Summary and conclusions

Early DD schemes were designed to remove unwanted system–bath interactions to a given, low order in time-dependent perturbation theory [3, 4]. CDD is the first explicit scheme proposed to remove such interactions to an arbitrary order,

via a recursive construction in which each successive level suppresses another order in time-dependent perturbation theory [6]. This work reports the first experimental demonstration of CDD, using NMR. As predicted, CDD outperforms PDD in preserving the fidelity of quantum states. The experimental system studied here—the ^{13}C spin qubit of adamantane—undergoes single-axis decoherence, so that one might suspect that the full CDD sequence we used is 'overkill' for this system, because this sequence was designed to suppress full three-axis decoherence. However, pulse errors and magnetic field inhomogeneity result in second-order off-axis contributions to decoherence, which is why DD sequences using just a single-pulse type (e.g. UDD) cannot be expected to perform well on our system. Nevertheless, it is important to identify an experimentally feasible NMR system where dephasing and longitudinal relaxation are of comparable magnitude, and to study the performance of CDD relative to other methods capable of suppressing full decoherence, such as QDD.

Appendix. Distance and fidelity

A distance measure between quantum states ρ and σ (density matrices) is provided by the 'trace-norm distance': $D(\rho, \sigma) \equiv \frac{1}{2}\|\rho - \sigma\|_1$, where $\|A\|_1 \equiv \text{Tr}\sqrt{A^\dagger A} = \sum_i s_i(A)$, and where $s_i(A)$ are the eigenvalues of $\sqrt{A^\dagger A}$. The trace norm distance is the maximum probability of distinguishing ρ from σ, vanishes if and only if $\rho = \sigma$, and is related to the fidelity $F(\rho, \sigma) \equiv \|\sqrt{\rho}\sqrt{\sigma}\|_1$ via $1 - D(\rho, \sigma) \leqslant F(\rho, \sigma) \leqslant \sqrt{1 - D^2(\rho, \sigma)}$, so that knowing one bounds the other. In the case of comparing an output state σ to a desired pure state $\rho = |\psi\rangle \langle\psi|$, this reduces to $F = \sqrt{\langle\psi| \sigma |\psi\rangle}$, and perfect fidelity ($F = 1$) results if and only if $\rho = \sigma$.

---

[7] We estimate $J \sim 600$ Hz and $\beta \sim 2.5$ kHz on the basis of a simulation: a spin system consisting of one ^{13}C and six ^{1}H with these parameters produced the best fit to the experimental free induction decay.

[8] We are taking some liberty here with the term 'fidelity': our theoretical analysis indeed provides a fidelity bound, while the experimental results report different, but related quantities, namely NMR signal and decoherence rate. Moreover, our experiment is restricted to testing the performance of CDD for a single input state, whereas the theoretical distance and fidelity measures we have discussed apply for general input states.

References

[1] Zurek W 1991 *Phys. Today* **44** 36
[2] Aharonov D and Ben-Or M 1996 *Proc. 37th Conf. on Foundations of Computer Science (FOCS)* (Los Alamitos, CA: IEEE Computer Society Press) p 46
[3] Viola L, Knill E and Lloyd S 1999 *Phys. Rev. Lett.* **82** 2417
[4] Zanardi P 1999 *Phys. Lett.* A **258** 77
[5] Viola L and Knill E 2005 *Phys. Rev. Lett.* **94** 060502
[6] Khodjasteh K and Lidar D A 2005 *Phys. Rev. Lett.* **95** 180501
[7] Uhrig G 2007 *Phys. Rev. Lett.* **98** 100504
[8] Santos L F and Viola L 2006 *Phys. Rev. Lett.* **97** 150501
[9] Zhang W, Konstantinidis N P, Dobrovitski V V, Harmon B N, Santos L F and Viola L 2008 *Phys. Rev.* B **77** 125336
[10] Yang W and Liu R-B 2008 *Phys. Rev. Lett.* **101** 180403
[11] Uhrig G S and Lidar D A 2010 *Phys. Rev.* A **82** 012301
[12] Biercuk M, Uys H, VanDevender A, Shiga N, Itano W and Bollinger J 2009 *Nature* **458** 996
[13] Biercuk M J, Uys H, VanDevender A P, Shiga N, Itano W M and Bollinger J J 2009 *Phys. Rev.* A **79** 062324

[14] Jenista E R, Stokes A M, Branca R T and Warren W S 2009 *J. Chem. Phys.* **131** 204510

[15] Ryan C A, Hodges J S and Cory D G 2010 *Phys. Rev. Lett.* **105** 200402

[16] Szwer D J, Webster S C, Steane A M and Lucas D M 2011 *J. Phys. B: At. Mol. Opt. Phys.* **44** 025501

[17] Ajoy A, Alvarez G A and Suter D 2011 *Phys. Rev.* A **83** 032302

[18] West J R, Fong B H and Lidar D A 2010 *Phys. Rev. Lett.* **104** 130501

[19] Wang Z-Y and Liu R-B 2011 *Phys. Rev.* A **83** 022306

[20] Ng H-K, Lidar D A and Preskill J P 2011 *Phys. Rev.* A **84** 012305

[21] West J R, Lidar D A, Fong B H and Gyure M F 2010 *Phys. Rev. Lett.* **105** 230503

[22] Khodjasteh K and Lidar D A 2007 *Phys. Rev.* A **75** 062310

[23] Witzel W M and Sarma S Das 2007 *Phys. Rev.* B **76** 241303

[24] Zhang W, Dobrovitski V V, Santos L F, Viola L and Harmon B N 2007 *Phys. Rev.* B **75** 201302

[25] Álvarez G A, Ajoy A, Peng X and Suter D 2010 *Phys. Rev.* A **82** 042306

[26] Tyryshkin A M, Wang Z, Zhang W, Haller E E, Ager J W, Dobrovitski V V and Lyon S A 2010 arXiv:1011.1903

[27] Wang Z, Zhang W, Tyryshkin A M, Lyon S A, Ager J W, Haller E E and Dobrovitski V V 2010 arXiv:1011.6417

[28] Barthel C, Medford J, Marcus C M, Hanson M P and Gossard A C 2010 arXiv:1007.4255

[29] Carr H and Purcell E 1954 *Phys. Rev.* **94** 630

[30] Mehring M and Waugh J 1972 *Rev. Sci. Instrum.* **43** 649

[31] Haubenreisser U and Schnabel B 1979 *J. Magn. Reson.* **35** 175

[32] Burum D P 1981 *Phys. Rev.* B **24** 3684

[33] Lidar D A, Zanardi P and Khodjasteh K 2008 *Phys. Rev.* A **78** 012308

[34] Aliferis P, Gottesman D and Preskill J 2006 *Quantum Inf. Comput.* **6** 97